

Heteroleptic Phosphorescent Iridium(III) Compound with Blue Emission for Potential Application to Organic Light-Emitting Diodes

Sihyun Oh, Narae Jung, Jongwon Lee, Jinho Kim, Ki-Min Park,[†] and Youngjin Kang*

Division of Science Education & Department of Chemistry, Kangwon National University, Chuncheon 200-701, Korea

*E-mail: kangy@kangwon.ac.kr

[†]Department of Chemistry and Research Institute of Natural Science, Gyeongsang National University, Jinju 660-701, Korea

Received August 2, 2014, Accepted August 26, 2014

Blue phosphorescent (**dfppy**)₂**Ir(mppy)**, where **dfppy** = 2',6'-difluoro-2,3'-bipyridine and **mppy** = 5-methyl-2-phenylpyridine, has been synthesized by newly developed effective method and its solid state structure and photoluminescent properties are investigated. The glass-transition and decomposition temperature of the compound appear at 160 °C and 360 °C, respectively. In a crystal packing structure, there are two kinds of intermolecular interactions such as hydrogen bonding (C-H...F) and edge-to-face C-H... π (py) interaction. This compound emits bright blue phosphorescence with λ_{max} = 472 nm and quantum efficiencies of 0.23 and 0.32 in fluid and the solid state. The emission band of the compound is red-shifted by 40 nm relative to homoleptic congener, **Ir(dfppy)**₃. The ancillary ligand in (**dfppy**)₂**Ir(mppy)** has been found to significantly destabilize HOMO energy, compared to **Ir(dfppy)**₃, (**dfppy**)₂**Ir(acac)** and (**dfppy**)₂**Ir(dpm)**, without significantly changing LUMO energy.

Key Words : Blue phosphorescence, Ancillary ligand, X-ray structure, Organic Light-Emitting Diodes (OLEDs)

Introduction

Recently, iridium(III) compounds with fluorinated main bipyridine ligand have attracted much attention due to their color purity and high external quantum efficiency in Organic Light-Emitting Diodes (OLEDs).¹ This class of iridium compounds can be divided into two groups: homoleptic such as **Ir(dfppy)**₃ (**dfppy** = 2',6'-difluoro-2,3'-bipyridine) or heteroleptic such as (**dfppy**)₂**Ir(L[^]X)** where (L[^]X) is an ancillary ligand, as shown in Chart 1.² Especially, heteroleptic Ir(III) emitters in OLEDs have many advantages such as easy tuning of emission energies and photophysical properties by the modification of ancillary ligand.³ Representative examples of ancillary ligand in heteroleptic Ir(III) compounds are chelating O[^]O and N[^]O. However, the ancillary ligand in heteroleptic Ir(III) compounds impose severe problems. During OLEDs operation, the cleavage of Ir-N or Ir-O bond occurs readily in the presence of proton, which originates from an adjacent hole injection material (PEDOT:PSS).⁴ This is often called acid induced degradation (AID). Henceforth, to avoid this degradation of iridium emitters in PHOLEDs (Phosphorescent Organic Light-Emitting Diodes), it is highly desirable that ancillary ligand in heteroleptic iridium compounds has the same chelating mode of main ligand. Moreover, reports for the synthetic details and the derivatives of heteroleptic Ir(III) compounds with the same chelating modes, Ir(C[^]N)₂(C[^]N)', are very scarce relative to those of Ir(C[^]N)₂(L[^]X).⁵ These facts prompted us to develop new iridium(III) compound possessing main fluorinated bipyridine and a different C[^]N ancillary ligand and to investigate the effect of ancillary ligand on

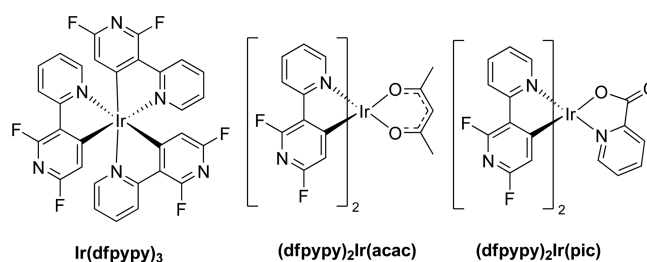


Chart 1. Representative examples of homoleptic and heteroleptic Ir(III) compounds based on bipyridine ligand.

photoluminescent properties. Herein, for potential application to OLEDs, we describe the results of our investigation on the preparation, crystal structure, photophysical properties of a novel iridium compound.

Experimental

General Considerations. All experiments were performed under a dry N₂ atmosphere using standard Schlenk techniques. All solvents were freshly distilled over appropriate drying reagents prior to use. All starting materials were purchased from either Aldrich or Strem and used without further purification. ¹H NMR spectra were recorded on a Bruker Avance 300 or 400 MHz spectrometer. UV-Vis spectra were obtained on a Varian Cary 50 UV/Visible spectrophotometer with all sample concentrations in the range of 10-50 μ M. Excitation and emission spectra were recorded on a Photon Technologies International QuantaMaster Model 2 spectrometer. Photoluminescent lifetimes were measured on a Photon

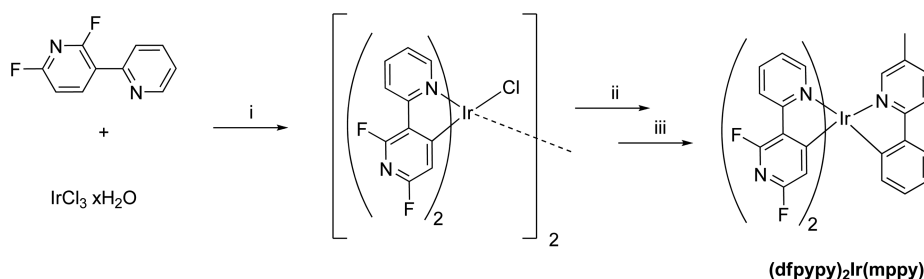
Technology International Phosphorescent lifetime spectrometer, Timemaster C-631F, equipped with a xenon flash lamp and digital emission photon multiplier tube for both excitation and emission. Cyclic voltammetry was performed using a BAS CV-50W voltammetric analyzer with scan rates of either 50 mV s^{-1} or 100 mV s^{-1} . The electrolytic cell used was a conventional three compartment cell with a Pt working electrode, Pt wire auxiliary electrode, and Ag/AgCl reference electrode. All experiments were performed at room temperature using $0.10 \text{ M NBu}_4\text{PF}_6$ as the supporting electrolyte in CH_3CN . All solutions for photophysical experiments were degassed for more than 30 min under N_2 . The thermogravimetric and DSC spectra were recorded on a Perkin-Elmer TGA-7 under nitrogen environment at a heating rate of $10 \text{ }^\circ\text{C/min}$ over a range of $25\text{--}700 \text{ }^\circ\text{C}$. The iridium dimer, $[(\text{dfppy})_2\text{Ir}(\mu\text{-Cl})]_2$,² and 5-methyl-2-phenylpyridine (mppy)¹² were synthesized according to previous reports.

X-ray Analysis. Single crystals of $(\text{dfppy})_2\text{Ir}(\text{mppy})$ suitable for X-ray analysis were obtained from slow vapor diffusion of hexane into a solution of $(\text{dfppy})_2\text{Ir}(\text{mppy})$ in dichloromethane. Single crystal diffraction data of $(\text{dfppy})_2\text{Ir}(\text{mppy})$ were collected on a Bruker Smart diffractometer equipped with a graphite monochromated $\text{Mo K}\alpha$ ($\lambda = 0.71073 \text{ \AA}$) radiation source, operating at 50 kV and 30 mA with a CCD detector. The 45 frames of two dimensional diffraction images were collected at room temperature and processed to obtain the cell parameters and orientation matrix. Decay was monitored by 50 standard data frames measured at the beginning and end of data collection. No significant decay was observed during the data collection. The frame data were processed to give structure factors using the SAINT-plus.¹³ Semi-empirical absorption corrections were applied to the data sets using the SADABS.¹³ The structure was solved by direct methods and refined by full matrix least squares methods on F^2 for all data using SHELXTL software.¹⁴ All non-hydrogen atoms of $(\text{dfppy})_2\text{Ir}(\text{mppy})$ were refined anisotropically. The hydrogen atoms were placed in calculated positions and refined using a riding model with isotropic thermal parameters 1.2 times those of the parent atoms. Crystallographic data for the structures reported here have been deposited with CCDC (Deposition No. CCDC-1015070). These data can be obtained free of charge via <http://www.ccdc.cam.ac.uk/conts/retrieving.html> or from CCDC, 12 Union Road, Cambridge CB2 1EZ, UK, E-mail: deposit@ccdc.cam.ac.uk

Synthesis of $(\text{dfppy})_2\text{Ir}(\text{mppy})$. Iridium dimer, $[(\text{dfppy})_2\text{Ir}(\mu\text{-Cl})]_2$ (1 g, 0.82 mmol), was dissolved in CH_2Cl_2 (125 mL). A methanol (1 mL) solution of silver tetrafluoroborate (0.32 g, 1.64 mmol) was added to iridium solution. The mixture was stirred for 5 h at room temperature under the dark, resulted in a gray AgCl precipitate. The reaction mixture was filtered over Celite to remove precipitate. The filtrate was evaporated *in vacuo* and then redissolved in ethanol (30 mL). An ethanol solution of 5-methyl-2-phenylpyridine (0.55 g, 3.28 mmol) was subsequently added. After reaction mixture was refluxed for 6 h, all solvent was removed under vacuum. The residues were purified by column chromatography using CH_2Cl_2 as an eluent. Yields: 25%. ^1H NMR (CD_2Cl_2) δ 8.29 (d, 1H, $J = 6.3 \text{ Hz}$), 8.24 (d, 1H, $J = 6 \text{ Hz}$), 8.13 (dd, $J = 4.5 \text{ Hz}$, $J = 0.9 \text{ Hz}$, 1H), 7.94 (d, 1H, $J = 6 \text{ Hz}$), 7.79–7.75 (m, 4H), 7.70 (dd, 1H, $J = 18.6 \text{ Hz}$, $J = 6.6 \text{ Hz}$), 7.64 (dd, 1H, $J = 6.3 \text{ Hz}$, $J = 0.6 \text{ Hz}$), 7.00 (td, 1H, $J = 17.7 \text{ Hz}$, $J = 0.6 \text{ Hz}$), 6.96–6.94 (m, 3H), 6.83 (dd, 1H, $J = 5.1 \text{ Hz}$, $J = 0.6 \text{ Hz}$), 6.08 (t, 1H, $J = 2.1 \text{ Hz}$), 5.78 (t, 1H, $J = 1.5 \text{ Hz}$). $^{13}\text{C}\{^1\text{H}\}$ NMR (CD_2Cl_2 , 100 MHz) δ 170.8, 165.4, 154.7, 153.7, 150.8, 150.4, 148.7, 145.3, 139.7, 139.2, 137.9, 137.5, 137.2, 136.7, 133.7, 132.2, 130.5, 128.9, 128.8, 126.8, 124.7, 123.6, 123.0, 119.8, 114.3, 109.3, 109.1, 107.3, 107.0, 18.2. MASS (MALDI-TOF): $m/z = 742$. Anal. Calcd for $\text{C}_{32}\text{H}_{20}\text{F}_4\text{IrN}_5$: C 51.75, H 2.71, N 9.43. Found: C 51.69, H 2.66, N 9.50.

Results and Discussion

Synthesis and X-ray Structure. The treatment of $[(\text{dfppy})_2\text{Ir}(\mu\text{-Cl})]_2$ with AgBF_4 in MeOH yielded the monomeric iridium precursor. Subsequently, the precursor was reacted with cyclometallating ligand, 5-methyl-2-phenylpyridine, to obtain desired compound in refluxing ethanol, as shown Scheme 1. By the reaction iridium dimer with Ag(I) as a chloride scavenger, the cleavage of Ir-Cl bond occurs effectively. This precursor is strongly solvated in coordinating solvents such as acetonitrile, dimethylformamide, methanol and dimethylsulfoxide to produce solvated mononuclear iridium compound.⁶ The solvated iridium compound readily undergo substitution reactions to give $(\text{dfppy})_2\text{Ir}(\text{mppy})$, because the solvent molecules coordinated to iridium ion are highly labile. This compound is soluble in common organic solvents except pentane and hexane and has been fully characterized by ^1H , ^{13}C NMR,



Scheme 1. Synthetic procedures for $(\text{dfppy})_2\text{Ir}(\text{mppy})$: i) 2-Ethoxyethanol: H_2O (3:1), $140 \text{ }^\circ\text{C}$, 14 h. ii) $\text{AgBF}_4/\text{CH}_2\text{Cl}_2$, MeOH, rt, 5 h. iii) 5-methyl-2-phenylpyridine/EtOH, reflux, 6 h.

elemental analyses and X-ray diffraction analysis. The ^1H NMR spectrum of $(\text{dfppy})_2\text{Ir}(\text{mppy})$ showed well resolved characteristic peaks from 5.5 and 8.5 ppm (see Supporting Information).

In order for compounds to be useful in OLEDs, they should be sufficiently thermally and morphologically stable.⁷ Therefore, we carried out both thermogravimetric analysis (TGA) and differential scanning calorimetry (DSC) experiments to investigate decomposition temperature and the glass-forming properties for this compound. The decomposition temperature of $(\text{dfppy})_2\text{Ir}(\text{mppy})$, which is defined as a 5% loss of weight, appeared at *ca.* 360 °C. This temperature is high enough to deposit molecules under reduced pressure without any degradation. However, it is significantly lower than that of homoleptic $\text{Ir}(\text{dfppy})_3$ (452 °C). This can be due to the lack of fluorine substituents in ancillary ligand. For DSC experiment, a glass transition (T_g) in the first heating cycle was observed at approximately 160 °C. Both TGA and DSC data are deposited in supporting information. Consequently, the high decomposition and glass transition temperature of $(\text{dfppy})_2\text{Ir}(\text{mppy})$ makes it potentially useful triplet emitter for applications in PHOLEDs.

The structure of $(\text{dfppy})_2\text{Ir}(\text{mppy})$ was unambiguously established by single-crystal X-ray diffraction analysis. Figure 1 shows the molecular structure of this compound. The X-ray crystallographic data are summarized in Table 1 and the selected bond lengths and bond angles are described in Table 2. Notably, there is a solvent molecule in the asymmetric unit. As shown by Figure 1, this compound has a distorted octahedral geometry with a facial configuration, which is a typical for phenylpyridine based organo-iridium(III) compounds.⁶ All σ -donor C atoms (C1, C13, and C23) in either metallated difluoronated pyridine or phenylpyridine ligands are located a *trans* position to dative N atoms (N2, N4, and N1) in the adjacent C^N ligands. The bond lengths of Ir-C are from 1.997(4) to 2.015(5), which are similar to those of $\text{Ir}(\text{dfppy})_3$. In addition, The Ir-N bond lengths (2.123(4)-2.134(4) Å) of $(\text{dfppy})_2\text{Ir}(\text{mppy})$ are in agreement with those of *fac*- $\text{Ir}(\text{flz})_3$ (2.095(7)-2.121(6) Å), and *fac*- $\text{Ir}(\text{ppz})_3$ (1-phenylpyrazoly-*N*, C2') (2.117(5)-2.135(5) Å).⁸ There are two kinds of the intermolecular interactions in

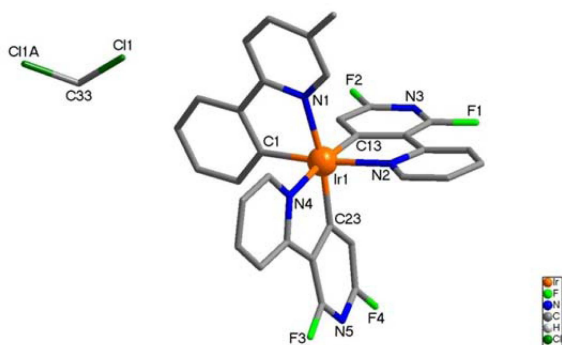


Figure 1. Molecular structure of $(\text{dfppy})_2\text{Ir}(\text{mppy})$, showing the atom-numbering scheme. The hydrogen atoms were omitted for clarity.

Table 1. Crystal data and structure refinement for $(\text{dfppy})_2\text{Ir}(\text{mppy})$

Compound	$(\text{dfppy})_2\text{Ir}(\text{mppy})$
Empirical formula	$[\text{Ir}(\text{C}_{10}\text{H}_5\text{N}_2\text{F}_2)_2(\text{C}_{12}\text{H}_{10}\text{N})] \cdot 0.5(\text{CH}_2\text{Cl}_2)$
Formula weight	785.19
Temperature	173(2) K
Wavelength	0.71073 Å
Crystal system, Space group	Orthorhombic, <i>Pbcn</i>
a, b, c (Å)	9.5727(2) Å, 17.4341(4) Å, 33.2626(6) Å
α, β, γ (°)	90°
Volume	5551.2(2) Å ³
Z, Density (calculated)	8, 1.879 Mg/m ³
Absorption coefficient	4.967 mm ⁻¹
<i>F</i> (000)	3048
Crystal size	0.31 × 0.13 × 0.11 mm ³
θ range for data collection	2.34 to 27.00°
Reflections collected	27149
Independent reflections	6048 [<i>R</i> (int) = 0.0322]
Final <i>R</i> indices [<i>I</i> > 2 σ (<i>I</i>)]	<i>R</i> ₁ = 0.0333, <i>wR</i> ₂ = 0.0713
<i>R</i> indices (all data)	<i>R</i> ₁ = 0.0416, <i>wR</i> ₂ = 0.0749
Absorption correction	Semi-empirical
Data / restraints / parameters	6048 / 0 / 393
Goodness-of-fit on <i>F</i> ²	1.076
Largest diff. peak and hole	1.243 and -1.977 e.Å ⁻³

crystal packing. One is weak hydrogen bonding such as C-H...F type. The distances of H...F is approximately 2.50 Å. The other is edge-to-face C-H... π (py) interactions, with the average distance of 2.85 Å (see Supporting Information). These intermolecular interactions may contribute to the stabilization of the crystal packing, in agreement with the result of the TGA experiment. Details for intermolecular interactions are deposited in Figure S5 of supporting information.

Photophysical and Electrochemical Properties. The UV/vis spectrum of this compound displays intense absorption bands ($\epsilon = 48,000$) ranging from 250 to 300 nm, indicating that electronic transitions are mostly ligand-centered (LC) π - π^* , originating from both phenylpyridyl and bipyridyl groups (Figure 2). Another weak absorption at 380 nm with $\epsilon = 7,200 \text{ M}^{-1} \text{ cm}^{-1}$ of molar extinction coefficient can be spin-allowed metal-to-ligand charge transfer ($^1\text{MLCT}$) transition. Next long tail extending to 450 nm is attributed to a mixed state involving both spin-orbit coupling enhanced ^3LC and $^3\text{MLCT}$ transitions. Although, the absorption pattern of $(\text{dfppy})_2\text{Ir}(\text{mppy})$ is very similar with that of $\text{Ir}(\text{dfppy})_3$, a weak and red-shifted $^1\text{MLCT}$ band compared to that of $\text{Ir}(\text{dfppy})_3$ ($\lambda = 360 \text{ nm}$, $\epsilon = 8,200 \text{ M}^{-1} \text{ cm}^{-1}$) was observed. This result can be attributed to the introduction of ancillary ligand, as well as the lack of fluorine substituents in ancillary.

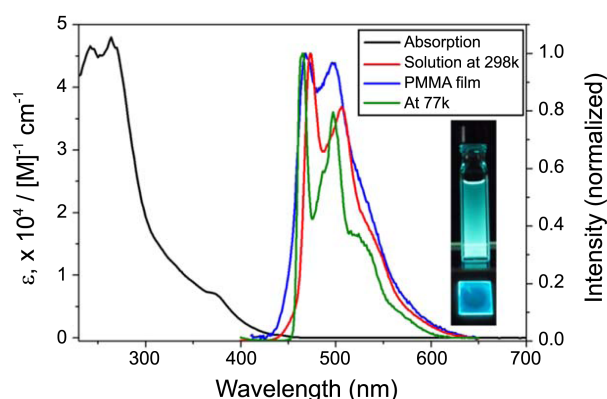
This compound has bright blue and well structured emission bands in solution at room temperature, with $\lambda_{\text{max}} = 472$ and 493 nm (Figure 2). The intensity at 493 nm, however, is much lower than at 472 nm. This highly structured emission band mainly originates from the $^3\pi$ - π^* state based on previ-

Table 2. Selected bond lengths (Å) and angles (°) of (dfppy)₂Ir(mppy)

Bond distances (Å)		Bond angles (°)	
Ir-C1	2.015(5)	C(23)-Ir(1)-C(13)	93.96(2)
Ir-C13	2.005(5)	C(23)-Ir(1)-C(1)	95.59(2)
Ir-C23	1.997(4)	C(13)-Ir(1)-C(1)	93.48(2)
Ir-N1	2.123(4)	C(23)-Ir(1)-N(1)	170.34(2)
Ir-N2	2.134(4)	C(13)-Ir(1)-N(1)	94.69(2)
Ir-N4	2.134(4)	C(1)-Ir(1)-N(1)	79.61(2)
		C(23)-Ir(1)-N(4)	79.95(2)
		C(13)-Ir(1)-N(4)	173.59(2)
		C(1)-Ir(1)-N(4)	89.12(2)
		N(1)-Ir(1)-N(4)	91.53(2)
		C(23)-Ir(1)-N(2)	88.40(2)
		C(13)-Ir(1)-N(2)	79.26(2)
		C(1)-Ir(1)-N(2)	171.96(2)
		N(1)-Ir(1)-N(2)	97.42(1)
		N(4)-Ir(1)-N(2)	98.46(2)

ous reports.^{1c} Therefore, the phosphorescent emission observed in (dfppy)₂Ir(mppy) is attributable to the ³π-π* with small contribution of the MLCT transition. In addition, the emission of (dfppy)₂Ir(mppy) does not change significantly with concentration in solution or from the solution to the solid state (10 wt %-PMMA film), indicating that there are little intermolecular interactions in the solid state. However, the thin film of (dfppy)₂Ir(mppy) exhibited slightly broader emission than in fluid state. The emission spectra of the compound at 77 K displays well resolved vibronic features along with a 8 nm blue-shifted emission energy in contrast to the spectrum at room temperature, as shown in Figure 2. This can be due to the rigidochromic effect.⁹ The triplet energy of the compound was estimated to be 2.67 eV, using emission maximum at 77 K. This value is similar than that of the standard sky-blue emitter Firpic (E_T = 2.7 eV). Indeed, due to the introduction of ancillary ligand, (dfppy)₂Ir(mppy) shows an remarkable red-shifted emission (more than 30 nm) in the fluid and solid states compared to homoleptic iridium(III) counterpart. The photoluminescence quantum yields (Φ_{PL}) of (dfppy)₂Ir(mppy) were estimated by using Firpic as a reference (Φ_{PL} = 0.6). The photoluminescence quantum yields in fluid state and the thin film are 0.23 and 0.32 respectively. This value is much lower than in Ir(dfppy)₃ (Φ_{PL} = 0.71). In general, if the triplet energy of main C[^]N ligand in the series of (C[^]N)₂Ir(L[^]X) is larger than that of ancillary(L[^]X), the emission of (C[^]N)₂Ir(L[^]X) results from an ancillary ligand-based excited state, giving rise to very inefficient phosphorescence.¹⁰ Therefore, deteriorated efficiency of (dfppy)₂Ir(mppy) can be due to ppy-based excited state, because the T₁ (2.6 eV) of ppy is smaller than that of fluorinated bipyridine (T₁ = ca. 2.9 eV).

To gain further insight into the relaxation dynamics of (dfppy)₂Ir(mppy), we measured phosphorescence lifetimes(τ). This compound showed single exponential decay profiles with the lifetimes of 2.7(1) μs at 298 K and 5.2(1)

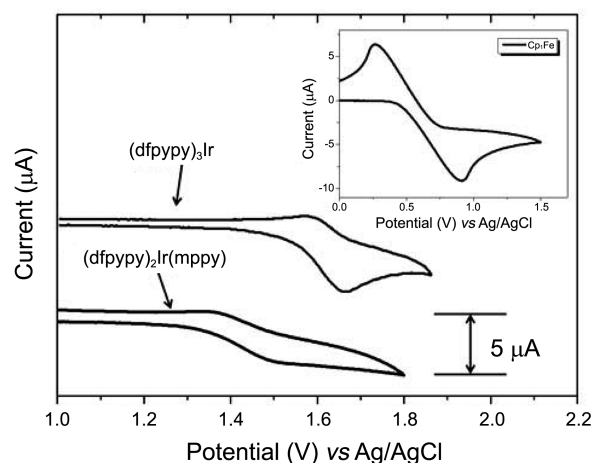
**Figure 2.** Absorption and emission spectra of (dfppy)₂Ir(mppy).

ms at 77 K, respectively. The radiative decay (*k*_r) and non-radiative decay (*k*_{nr}) rate constants (× 10⁵) were determined to be 0.8 and 2.8, respectively, using following two Eqs. (1) and (2).

$$\Phi_{\text{PL}} = k_r / (k_r + k_{nr}) \quad (1)$$

$$1/\tau = k_r + k_{nr} \quad (2)$$

Interestingly, the *k*_{nr} value of (dfppy)₂Ir(mppy) is similar with that of (dfppy)₂Ir(dpm) (2.3 × 10⁵ s⁻¹), whereas the *k*_r value is almost four-times smaller than that of (dfppy)₂Ir(dpm) (3.2 × 10⁵ s⁻¹).² These results strongly indicate that the ppy unit as an ancillary significantly retards the radiative decay process, leading to deteriorated PL efficiency. To estimate HOMO energy of (dfppy)₂Ir(mppy) and investigate the electrochemical behavior caused by ppy ancillary ligand, cyclic voltammetry(CV) experiment was performed. In addition, CV work for homoleptic Ir(dfppy)₃ was also carried out under the same experimental conditions for the purpose of comparison. A (dfppy)₂Ir(mppy) showed a single quasi-reversible oxidation at *E*_{onset} = 0.86 V (vs. Fc/Fc⁺, ferrocene/ferrocenium). As shown in Figure 3, the oxidation potential of (dfppy)₂Ir(mppy) is much lower than that of Ir(dfppy)₃, while this value is comparable to

**Figure 3.** Comparison of oxidation potentials (vs Ag/AgCl in CH₃CN) of (dfppy)₂Ir(mppy) and Ir(dfppy)₃ under the same condition (Inset: Standard Fc/Fc⁺).

that of (MeO₂ppy)₂Ir(pic).^{5c} Using an oxidation potential of ferrocene/ferrocenium (4.8 eV below the vacuum level),¹¹ the HOMO level was deduced to be −5.66 eV, which is dramatically higher than those of iridium(III) analogues, Ir(dfppy)₃ (HOMO = −6.39 eV), (dfppy)₂Ir(pic) (HOMO = −6.14 eV). This observation implies that the HOMO energy level has been increased by ancillary ligand.

The LUMO level was estimated to be −2.77 eV from the onset potential of reduction ($E_{\text{onset}} = -2.03$ V vs Fc/Fc⁺). Although the triplet levels of the ancillary ligand such as acac(acetylacetone) and dpm(dipivaloylmethane) lie well above that of dfppy main ligand, the LUMO energy of (dfppy)₂Ir(mppy) is very similar to those of (dfppy)₂Ir(acac) and (dfppy)₂Ir(dpm). Therefore, it is noteworthy that ppy ancillary ligand with low-lying triplet energy level compared to main dfppy ligand has great influence on the HOMO energy level in fluorinated bipyridine based Ir(III) derivatives.

Conclusion

A heteroleptic cyclometallated iridium(III) compound, (dfppy)₂Ir(mppy), possessing dfppy as main ligands and mppy as an ancillary was synthesized by using Ag(I). This compound showed facial configuration in crystal structure and high thermal stability with more than 300 °C of decomposition temperature. In photophysical properties, a (dfppy)₂Ir(mppy) shows a remarkable ~30 nm red-shifted emission in the fluid and solid states compared to homoleptic iridium(III) counterpart. This fact implies that ppy ancillary ligand plays an important role in the red-shifted emission of (dfppy)₂Ir(mppy). In addition, a dramatically higher HOMO energy relative to its iridium analogues was observed. Therefore, the color tuning in dfppy-based iridium(III) compounds could be achieved by judicious selection of a different ancillary ligand with the same C[^]N chelating mode of main ligand. High thermal stability, moderate phosphorescent quantum efficiency and reversible oxidation make (dfppy)₂Ir(mppy) a suitable triplet emitter for use in blue PHOLEDs. Further study on OLEDs performance using this compound is currently being investigated in our laboratory.

Acknowledgments. This research was supported by the Basic Science Research Program through the National Re-

search Foundation of Korea (NRF), funded by the Ministry of Education, Science and Technology (2011-0010518), and the industrial strategic technology development program (10039141), funded by the Ministry of Trade, Industry & Energy (MOTIE, Korea).

References

- (a) Lee, S. J.; Park, K.-M.; Yang, K.; Kang, Y. *Inorg. Chem.* **2009**, *48*, 1030. (b) Park, J.; Oh, H.; Oh, S.; Kim, J.; Park, H. J.; Kim, O. Y.; Lee, J. Y.; Kang, Y. *Org. Electron.* **2013**, *14*, 3228. (c) Jung, N.; Lee, E.; Kim, J.; Park, H.; Park, K.-M.; Kang, Y. *Bull. Korean Chem. Soc.* **2012**, *33*, 183. (d) Yang, C.-H.; Mauro, M.; Polo, F.; Watanabe, S.; Muenster, I.; Fröhlich, R.; De Cola, L. *Chem. Mater.* **2012**, *24*, 3684. (e) Kessler, F.; Costa, R. D.; Di Censo, D.; Scopelliti, R.; Orti, E.; Bolink, H. J.; Meier, S.; Sarfert, W.; Grätzel, M.; Nazeeruddin, M. K.; Baranoff, E. *Dalton Trans.* **2012**, *41*, 180.
- Kang, Y.; Chang, Y.-L.; Lu, J.-S.; Ko, S.-B.; Rao, Y.; Varlan, M.; Lu, Z.-H.; Wang, S. *J. Mater. Chem. C* **2013**, *1*, 441.
- Oh, H.; Park, K.-M.; Hwang, H.; Oh, S.; Lee, J. H.; Lu, J.-S.; Wang, S.; Kang, Y. *Organometallics* **2013**, *32*, 6427.
- Schmidbauer, S.; Hohenleutner, A.; König, B. *Adv. Mater.* **2013**, *25*, 2114.
- (a) Yersin, H. *Highly Efficient OLEDs with Phosphorescent Materials*; Wiley-VCH: Weinheim, Germany, 2008. (b) Yun, C.; Chou, P.-T. *Chem. Soc. Rev.* **2010**, *39*, 638. (c) Ho, C.-L.; Wong, W.-Y. *New J. Chem.* **2013**, *37*, 1665. (d) Xu, H.; Chen, R.; Sun, Q.; Lai, W.; Su, Q.; Huang, W.; Liu, X. *Chem. Soc. Rev.* **2014**, *43*, 3259. (e) Lee, J.; Oh, H.; Kim, J.; Park, K.-M.; Yook, K. S.; Lee, J. Y.; Kang, Y. *J. Mater. Chem. C* **2014**, *2*, 6040.
- McGee, K. A.; Mann, K. R. *Inorg. Chem.* **2007**, *46*, 7800.
- Kessler, F.; Watanabe, Y.; Sasabe, H.; Katagiri, H.; Nazeeruddin, M. K.; Grätzel, M.; Kido, J. *J. Mater. Chem. C* **2013**, *1*, 1070.
- Sajoto, T.; Djurovich, P. I.; Tamayo, A.; Yousufuddin, M.; Bau, R.; Thompson, M. E.; Holmes, R. J.; Forrest, S. R. *Inorg. Chem.* **2005**, *44*, 7992.
- Tsuboyama, A.; Iwawaki, H.; Furugori, M.; Mukaide, T.; Kamatani, J.; Igawa, S.; Moriyama, T.; Miura, S.; Takiguchi, T.; Okada, S.; Hoshino, M.; Uenno, K. *J. Am. Chem. Soc.* **2003**, *125*, 12971.
- Lamansky, S.; Djurovich, P.; Murphy, D.; Razzaq, F. A.; Lee, H. E.; Adachi, C.; Burrows, P. E.; Forrest, S. R.; Thompson, M. E. *J. Am. Chem. Soc.* **2001**, *123*, 4304.
- Park, H.; Rao, Y.; Varlan, M.; Kim, J.; Ko, S.-B.; Wang, S.; Kang, Y. *Tetrahedron* **2012**, *68*, 9278.
- Liu, C.; Yang, W. *Chem. Commun.* **2009**, 6267.
- Bruker, SMART and SAINT: *Area Detector Control and Integration Software Ver. 5.0*; Bruker Analytical X-ray Instruments: Madison, Wisconsin, 1998.
- Bruker, SHELXTL: *Structure Determination Programs Ver. 5.16*; Bruker Analytical X-ray Instruments: Madison, Wisconsin, 1998.